Hydrogen absorption by thin Pd/Nb films deposited on glass

G. Reisfeld, Najeh M. Jisrawi, M. W. Ruckman, and Myron Strongin
Physics Department, Brookhaven National Laboratory, Upton, New York 11973
(Received 16 May 1995; revised manuscript received 10 November 1995)

Hydrogen absorption by 200–2000-Å-thick Pd-capped Nb films, between 5 and 110 °C, was studied by simultaneous four-probe resistivity and volumetric measurements. The resistivity as a function of hydrogen concentration was measured while charging the films with hydrogen, and was used to compute the change in hydrogen concentration in the film, during the reaction with oxygen. For the thinnest films (200 Å thick), the hydrogen charging and discharging curves indicate that a first-order gas-liquid-like phase transition with a T_c of 70–75 °C takes place. The H-Nb phase diagram for the 200-Å film looks like the H/bulk Nb α-α' phase diagram which has a higher T_c (173 °C). We attribute the substantial modifications of the film's phase diagram to the clamping of the Nb film at its interfaces with glass and Pd and to the nanostructure of the films.

I. INTRODUCTION

The absorption of hydrogen by metals has been studied by many techniques in the last four decades. It was found that, due to coherent metal crystal structure, the hydrogen absorption properties are influenced by the macroscopic geometry of the metal.[1] The modification of the absorption properties is even more extreme as the structure of the hydride becomes more two dimensional, (i.e., as in a thin film), or nanostructured (i.e., as in fine grained materials). For example, in the case of Nb films[2–5] and nanostructured Nb,[6] suppression of the hydride β phase is observed. The modification of the hydrogen phases in the thin films was attributed to the clamping of the film at the interfaces by the substrate, and probably the Pd overlayer. In addition, the same modification for the nanostructured Nb was attributed to the relaxation of the strain field within the grain boundaries. Until recently, one of the major gaps in our knowledge of hydrogen in thin Nb films was the lack of a direct measurement of hydrogen concentration in the films. This quantity was usually deduced indirectly from resistivity[5] measurements, or by lattice parameter changes.[7] In previous experiments a linear dependence of the resistivity on the hydrogen concentration was assumed.[5] This assumption is, of course, questionable when the hydrogen goes through phase transitions in the films. From structural measurements it was found that the lattice parameter changes are intrinsically different for films and bulk materials.[8] In 1993 Steiger and co-workers[2–4] reported direct measurements of hydrogen concentration in Nb films, epitaxially grown on sapphire, by using the well-known $^1H(^{15}N,\alpha\gamma)^{12}C$ nuclear reaction analysis (NRA) technique. Apart from measuring the total hydrogen content in the film, NRA can also provide a depth profile of the hydrogen concentration with a depth resolution of ~75 Å. Drawbacks in using NRA to study hydrogen absorption in thin films include the need to provide strong differential pumping (due to the ^{15}N beam line vacuum needs), which limits the hydrogen pressure in the sample cell to a maximum of 1 mbar. At these low pressures the hydrogen uptake rate is very slow for room temperature, and therefore the experiments were performed at temperatures above 166 °C. Another problem in applying NRA to study hydrogen in thin films is the removal of hydrogen from the sample by the ^{15}N beam.

The simplest way of measuring hydrogen uptake by a metal is the volumetric method. This simple technique has been used numerous times to study bulk materials, but has not been used to study gas uptake by thin Nb films. This method can be made even more powerful by the addition of the resistivity measurement. The lack of use of this technique is surprising since the measurement can be performed to a very high precision with a simple inexpensive apparatus. For instance, for 200-Å-thick films we could measure the hydrogen concentration up to a precision of one part in 10 000.

II. EXPERIMENTAL PROCEDURES

The samples were made by dc magnetron sputtering. The sputtering equipment was installed in a stainless-steel vacuum system that had both turbomolecular and cryopumping sufficient to achieve a base pressure of $\sim 2\times10^{-8}$ Torr when cryopumped or $\sim 2\times10^{-7}$ Torr when turbo-pumped. This drag turbo-pump remains on during sputtering when the Ar pressure is increased to 5×10^{-3} Torr. The sample substrate was a thin microscope glass (1×1 in.^{2}) that was acid washed and blow dried using nitrogen gas. The glass pieces were mounted on a rotating disk, and moved, within 10 s, from the position above the Nb magnetron gun to the position above the Pd gun (the deposition rate of Nb and Pd was ~10 Å/s). All the Nb films had a Pd overlayer thickness of ~100 Å to protect the Nb from oxidation, and to provide a high hydrogen uptake rate.[9] The impurity level of Nb was estimated by comparing the superconducting transition temperature T_c of the films with that of clean bulk Nb, nominally given as $T_c \sim 9.2$ K. For a typical 800-Å Nb thick film, the critical temperature was 8.8 K. A further estimate of the impurity level was deduced from the resistance ratio of the films between room temperature and 20 K. The resistivity ratio for all films was between 1.8 and 3. The two results imply an impurity level of less than 1 at %.

X-ray diffraction was used to determine the morphology and structure of the films. θ:2θ scans showed that both the Pd and Nb films grow with a preferred cyrstallographic orientation parallel to the substrate[5] (for Nb it is [110] planes, and for Pd the [111] planes). From the width of the Bragg peaks,

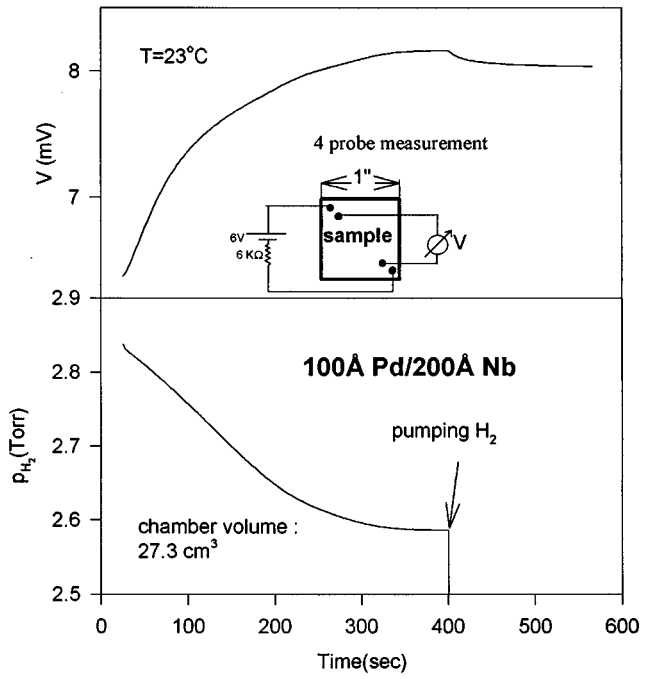

FIG. 1. Simultaneous measurements of the hydrogen uptake (bottom graph) and voltage change (top graph) of the film. The film was connected to a current source (inset). Note that pumping out H_2 produces an extremely slow discharge rate.

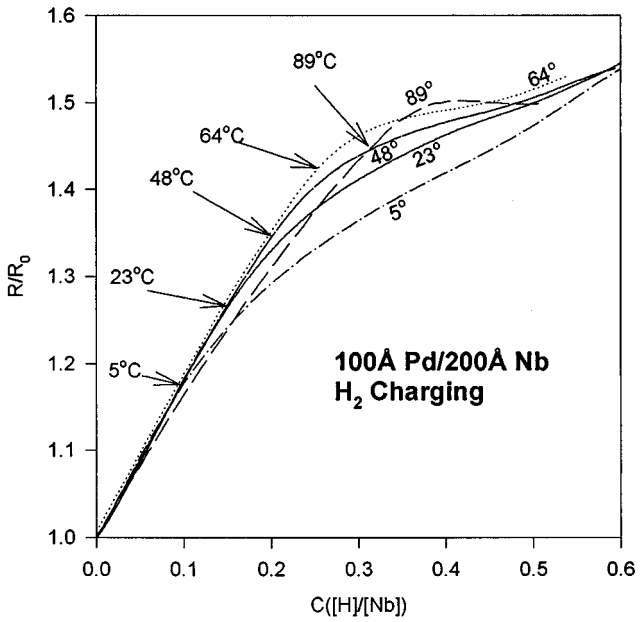

FIG. 2. The calculated normalized resistivity as a function of hydrogen concentration, for different temperatures. The arrows are pointing to the points at which each of the curves is no longer linear (The corresponding concentrations to the 5, 23, 48, 64, and 89 °C are $C=0.10$, 0.15, 0.20, 0.25, and 0.31.) The curve plotted for $T=23$ °C was processed from the data in Fig. 1.

the particle size was determined to be ~70 Å for the 200-Å Nb films.[10] The particle size increases with film thickness from 70 to ~150 Å for films going from 200- to 2000-Å thickness.[10] The size of the particles was found to be about the same both perpendicular and parallel to the plane of the substrate. The rotational orientation of the particles in the plane of the film was virtually random.[10] When the films were repeatedly cycled with hydrogen, the particle size decreased by ~20%; repeated cycling also stabilized the film's resistivity. Therefore, the results reported, hereon, are from films stabilized by repeated cycling.

The hydrogen uptake chamber was equipped with a pressure transducer (MKS type 122A) which measures pressures up to 10 Torr with a precision of 10^{-3} Torr. Another pressure transducer (MKS 315BHS-1000SPMC up to 1000 Torr) was used to measure the pressure of oxygen let into the chamber for discharging the films. The latter transducer was isolated from the chamber while charging the films. Four metal probes for the resistivity measurement were attached to the sample by means of springs, which were mounted on ceramic feedthroughs soldered to a KF40 flange. The sample was confined in the space made by an aluminum *O* ring connecting this flange and another KF40 flange. The chamber volume was 27.3 cm^3. The pumping unit was a turbomolecular station, and the chamber leak rate was estimated to be $\sim 10^{-3}$ Torr/min. The impurity level of hydrogen and oxygen used in the course of the experiments was ~10 ppm. The four probe measurements were carried out with a 1-mA current source (shown schematically in Fig. 1). For the voltage measurements, we used a Keithley 181 nanovoltmeter. The samples were moved from the sputtering chamber to the hydrogen uptake chamber in air.

III. RESULTS AND DISCUSSION

Figure 1 shows typical pressure and voltage (i.e., voltage drop across the sample) data recorded for a Pd-coated Nb film during hydrogen uptake. A family of such normalized (to the uncharged film) resistivity vs hydrogen concentration curves for different temperatures is shown in Fig. 2 (note that the curve scanned at 23 °C corresponds to the raw data of Fig. 1). The hydrogen concentration in the films was deduced from the change in the hydrogen gas pressure under the assumptions that the hydrogen gas is ideal, and that the Pd layer hydrogen concentration is negligible[11] (at our hydrogen pressure of less than 3 Torr). The assumption about the Pd layer was checked by doing the type of measurement shown in Fig. 1 on a film of pure Pd. The calculated resistivity curves in Fig. 2 are for the net Nb layer after a correction for the Pd film (the resistivity of the Nb is in parallel with that of the Pd). We assumed a constant resistivity of 20 $\mu\Omega$/cm for the Pd during the experiments. The resistivity of the uncharged Nb film was taken to be 30 $\mu\Omega$/cm. This value is consistent with the measured resistivity ratio of 2 for these films between room temperature and ~20 K. The initial resistivity trend of all the curves shown in Fig. 2 is linear with the hydrogen concentration, with a slope of ~2. This value is reproducible up to 1% for each specific film, but varies between different films by as much as 20%. The variation between different films originates from the fluctuations in the resistivity ratio (room temperature to 20 K for the uncharged film) between different films. For a resistivity ratio of 2, the initial slope in Fig. 2 (slope$\cong$2) implies a Nb resistivity vs hydrogen concentration of 0.6 $\mu\Omega$/(cm %[H]/[Nb]). This value is in agreement with the bulk value for low hydrogen concentrations[5] (0.64 $\mu\Omega$/(cm %[H]/[Nb])).

Each of the curves in Fig. 2 deviates from linearity at a different point (marked with arrows). For measurements at higher temperature the points of deviation have higher hydrogen concentration values. We attribute these inflection points to *the beginning of correlations between the hydrogen atoms*. According to the Drude model,[12] which ignores correlations, the resistivity of a metal should vary linearly with the number of scattering centers, which is, in this case, the number of hydrogen atoms.

Having presented evidence of H-H correlation, the emphasis of the paper now shifts to the nature of the correlated state, and how the data can provide more information about thermodynamic state variables like the chemical potential μ. As mentioned in the preceding discussion of the experiment, resistivity vs concentration curves were used to determine the hydrogen concentration while discharging the films with oxygen. The curve that was used for each discharge experiment was constructed during the charging process of the same cycle. This determination is based on the assumption that there is no hysteresis in the resistivity vs concentration curves. This assumption is justified by the extremely fast diffusion rate of hydrogen in the films (i.e., if a bulk diffusion rate is assumed, then hydrogen diffuses through 200-Å Nb in approximately 10^{-6} s). Therefore, within the time resolution of the measurements, hydrogen is in thermal equilibrium in the film. We also verified the existence of hydrogen equilibrium by measuring the resistivity vs hydrogen concentration while charging a film under different hydrogen pressures: The charging rate was found to be linear with hydrogen pressure. On the other hand, resistivity vs hydrogen concentration curves did not depend on the hydrogen pressure. Figure 3 shows the rate of hydrogen desorption vs the hydrogen concentration as a function of temperature deduced for a 200-Å Nb film. The measurements were performed under constant oxygen pressure (oxygen speeds up hydrogen desorption process by associating with hydrogen and forming water which desorbs from the surface). The rate of hydrogen desorption is simply the negative of the derivative of the hydrogen concentration with time $(-dc/dt)$. Because of the high precision of the resistivity measurement, the derivative was calculated directly, and no mathematical filters were used. The frequency of the data sampling was 0.2 Hz for all curves shown in Fig. 3. Estimating the rate of hydrogen desorption is much more precise for 200-Å Nb films than for thicker ones, due to the fact that for thicker films the resistivity is slowly changing for hydrogen concentrations greater than ~0.2. The precision of the estimate of hydrogen concentration is therefore much poorer for thick films.

A simple model is now presented which predicts that the *logarithm of the rate of hydrogen desorption* $(-dc/dt)$ *is proportional to the chemical potential* of hydrogen in the thin film. When hydrogen reacts with oxygen at the surface to form water, it has to come to the surface. Let the binding energy of the surface sites for hydrogen be E_{ad}, and the chemical potential of the hydrogen in the bulk and the surface be μ. Since hydrogen is in thermal equilibrium in the film, the hydrogen surface coverage θ_H is given by the expression:

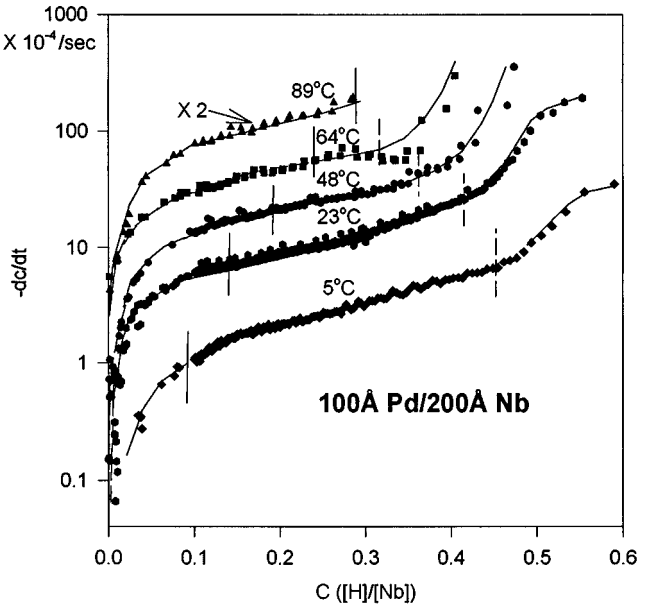

FIG. 3. The rate of hydrogen desorption $(-dc/dt)$ during exposure to oxygen. The oxygen pressure was 200 Torr for the curves corresponding to 5–64 °C, and 100 Torr for the curves corresponding to 89 °C (this curve was multiplied by a factor of 2, for the convenience of presentation. This multiplication merely shifts the curve up because of the logarithmic scaling). The vertical solid line in each curve marks the concentration at which above the absorbed hydrogen is correlated, as deduced from Fig. 2 (see the arrows in Fig. 2). The dashed vertical lines represent the transition to the liquid phase.

$$\theta_H = \frac{1}{1+e^{(E_{\mathrm{ad}}-\mu)/kT}}. \tag{1}$$

The curves shown in Fig. 3 indicate that the sample spontaneously discharges some of its hydrogen during the pumping out of the hydrogen used for charging. Figure 4 shows the spontaneous discharge of hydrogen for the room-temperature run. As can be seen, the rate of hydrogen desorption is dramatically reduced after the spontaneous discharge, where only a small amount of hydrogen comes out of the sample. Thus by the time oxygen is let into the chamber the surface coverage of hydrogen is much smaller than unity, and Eq. (1) can be replaced by the Maxwell distribution

$$\theta_H = e^{\mu/kT} \cdot e^{-E_{\mathrm{ad}}/kT}. \tag{2}$$

Let us further assume that, at a constant oxygen pressure, $-dc/dt$ is proportional to any power n (order of desorption) of θ_H. This assumption holds if the lateral interaction between surface hydrogen atoms is neglected, which is a reasonable scenario since the hydrogen coverage θ_H is very low. Thus $-dc/dt$ is expected to be proportional to $e^{\mu n/kT}$. Figure 3, accordingly, is a representation of the chemical potential for hydrogen in a 200-Å Nb film. The curves shown in Fig. 3 resemble the curves usually seen for first-order gas-liquid transitions, with one difference. The theoretical chemical potential for a mixed-phase region normally does not depend on the hydrogen concentration, while segments, corresponding to the mixed-phase region, of our curves in Fig. 3 are slightly inclined. Using the data in Figs. 2 and 3 we proceed

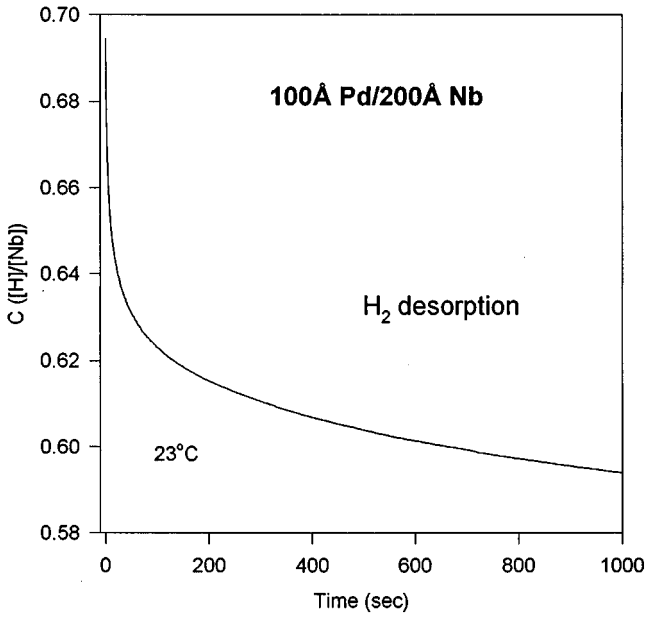

FIG. 4. The concentration of hydrogen in a thin film as a function of time, after charging the film to a concentration of ~0.7 and exposing it to vacuum.

to construct a H-Nb phase diagram. Figure 5 is a plot of the H-Nb phase diagram for a 200-Å Nb film as derived from data in Figs. 2 and 3. The points on the left-hand side of the curve mark the boundary between the low-density phase and the mixed phase deduced from Fig. 2 (marked as arrows in Fig. 2, and also the solid vertical lines in Fig. 3). The border between the mixed phase and the high-density phase (dashed vertical lines in Fig. 3) was taken as the concentration above which the slope of the parallel segments in Fig. 3 starts to increase rapidly.

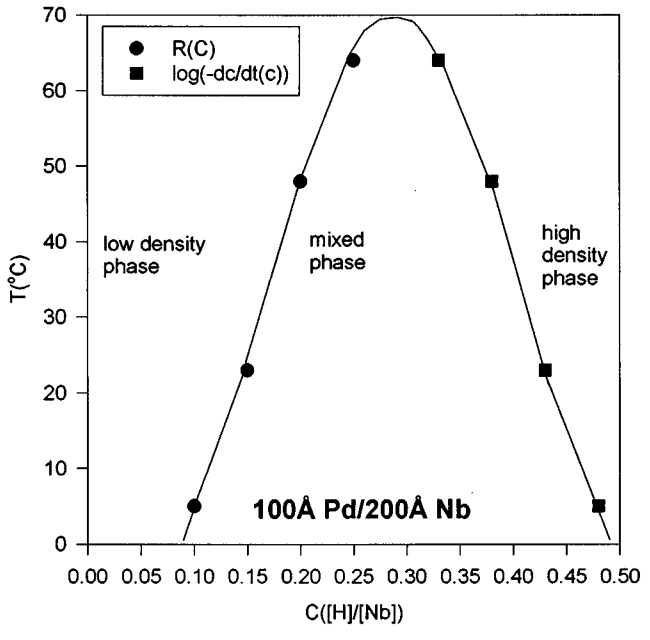

FIG. 5. Hydrogen phase diagram for 200-Å Nb. The points marking the border between the low-density phase and the mixed phase were deduced from Fig. 2 (marked as arrows in Fig. 2, and also solid vertical lines in Fig. 3). The border between the mixed phase and the high-density phase (dashed vertical lines in Fig. 3) was taken as the concentration above which the parallel segments in Fig. 3 deviate from linearity.

Figure 5 shows that the mixed-phase region has a T_c of 70–75 °C. This value is much lower than the bulk value [173 °C (Ref. 13)] which is observed for the α-α' phases. X-ray measurements performed on the these films[10] show a distortion of the Nb lattice, perpendicular to the substrate, while charging with hydrogen, and only a negligible distortion in the plane of the surface, up to about [H]/[Nb]~0.5. Figure 6 shows a set of x-ray θ:2θ scans, normal to a 100-Å Pd/600-Å Nb film [Fig. 6(a)], and almost in-plane of the film [Fig. 6(b)]. In Fig. 6(a), **q** (the reflected vector minus the incident vector) is directed to the normal of the film surface, and in Fig. 6(b) the angle between **q** and the surface normal is 85°. Figure 6(b) is therefore mainly affected by the in-plane lattice constants. Each scan was taken at a different time after a film charged with hydrogen was exposed to air. The scan marked with *A* was taken a few minutes after pumping the hydrogen used for charging (10 Torr), but before exposing the sample to air. Scan *B* was taken 45 min after the exposure to air, and scan *C* after 100 min. Each of the curves contains a peak associated with the Pd overlayer. As mentioned above, this peak is unchanged (see Fig. 6) during the discharge process, due to the negligible hydrogen concentration in the Pd. On the other hand, as expected, the Nb peaks vary during hydrogen discharging. An estimate of the hydrogen concentration in the Nb layer, corresponding to each one of the scans, is 0.55, 0.27, and 0.04 for *A*, *B*, and *C*, respectively. This estimate is based on the lattice parameter changes, assuming the bulk relation between hydrogen concentration and the volume change of the Nb unit cell ($\Delta V/V = 0.174 C_H$). As mentioned above, this estimate may not be precise for thin films.[8] In each of scans *A* and *C*, only one Nb peak in the [110] exists in Fig. 6(a), while in scan *B* there are two peaks. Scans *A* and *C* show the existence of pure phases, and scan *B* is consistent with the coexistence of the phases. For films thicker than 400-Å Nb, the two peaks representing the two coexisting phases are clearly resolved, and can be seen simultaneously (for the 200-Å films the resolution is limited by the particle size). In analogy to the bulk we call the low- and high-density phases α and α', although we emphasize that we know little about the high-density phase. The modifications in lattice geometry are due to clamping. As can be seen in Fig. 6(b), x-ray scattering results in the 600-Å films show almost no expansion in the plane of the film up to [H]/[Nb]~0.5. However, in somewhat thicker films, or at higher hydrogen concentrations, we do see expansion in the plane of the film, and the effect of clamping is smaller. This is no doubt related to the work of Miceli *et al.*,[14] where this kind of phenomenon was studied in thin Nb films and Nb/Ta superlatices epitaxially grown on sapphire. In the case of the Nb/sapphire films,[14] clamping of the films was observed only at low hydrogen concentration. At higher concentrations, near [H]/[Nb]~0.1, the clamping was removed, and two phases with equal density were developed. In contrast, in our case, the 200-Å Nb film is always clamped, and the different phases have different densities.

As was discussed above, the inclination of the segments in the curves of Fig. 3 corresponding to the mixed-phase

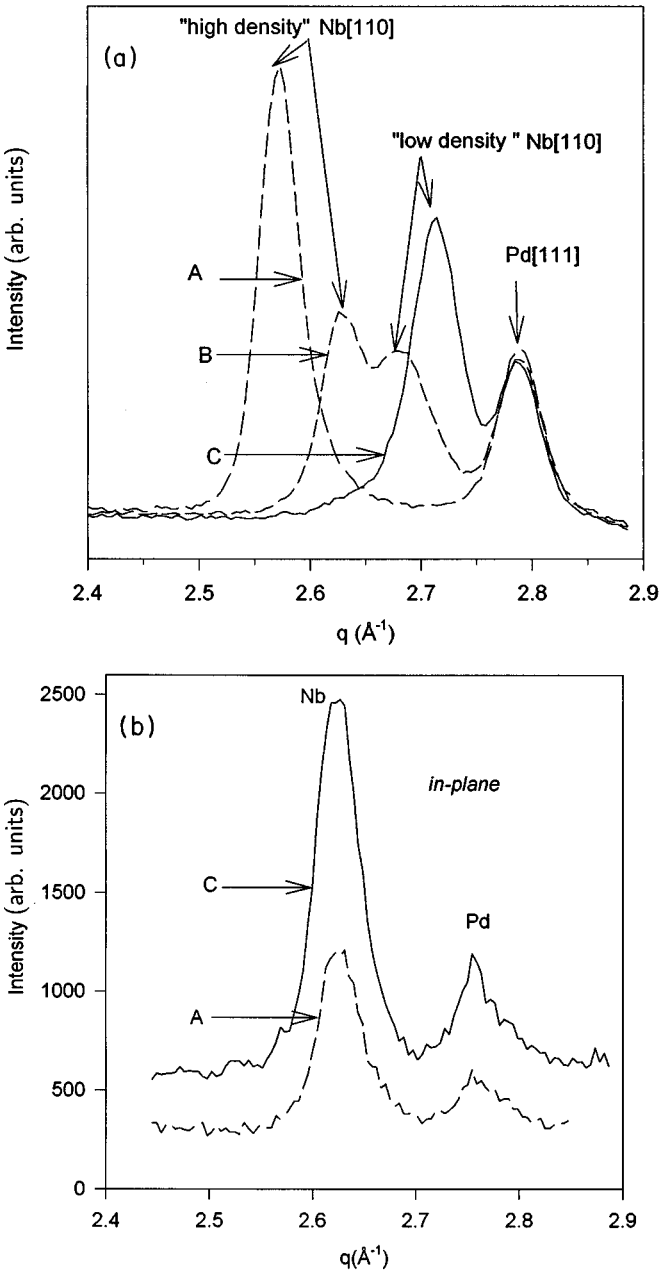

FIG. 6. X-ray θ:2θ scans of a 100-Å Pd/600-Å Nb film. In (a), q is directed to the normal of the film surface, and (b) the angle between q and the surface normal is 85°. Each scan was taken at a different time, after a film charged with hydrogen was exposed to air: *A*—a few minutes after pumping the hydrogen used for charging (10 Torr) and before exposing the sample to air (C([H]/[Nb])~0.55). *B*—45 min after exposure to air (C([H]/[Nb])~0.27). *C*—100 min after exposure to air (C([H]/[Nb])~0.04).

region is not seen during bulk experiments. Also, x-ray studies made on these films[10] have shown that, in the mixed-phase region, the centroid of Bragg peaks for the H-Nb phases moves slightly with decreasing or increasing H concentration. We associate these features with the macroscopic structure of the films. We propose the following dynamic picture for the thermal H-Nb equilibrium in the two-phase region: The hydrogen atoms diffuse between particles. In the process of diffusing from one particle to another, the hydrogen may flip the particles from one phase to the other. The grain boundaries act to disconnect the strain field between particles, leaving diffusion as the only communication channel. The fact that in thicker films (where there is adequate x-ray sensitivity) the mixed phase can be resolved implies that each particle has only one H-Nb phase. If each particle contained two phases concurrently, the Bragg peaks would have been unresolved, because the particle structure would be incoherent or the domains would be too small. If the strain field is completely released between particles, then we would expect to have no correlations between the phases in adjacent particles. Conversely, if the strain field is not completely damped, then we may expect clusters of particles with the same phase. We cannot judge from our measurements which of the above actually occurs.

$-dc/dt$ (which is related to the chemical potential) and the angular position of the two x-ray peaks are not constant in the two-phase region, because of the macroscopic inhomogeneous structure of the films (i.e., different regions of the films may have a slightly different structure).

A lowering of T_c in thin Pd films was also reported by Feenstra *et al.*[15] for thin films of Pd. The lowering of T_c implies a smaller H-H interaction[16] in the films, which can be expressed as a further modification of the chemical potential μ.[17] This is given by

$$\mu=\mu_0-uC+kT\ \ln\left(\frac{C}{1-C}\right), \tag{3}$$

where uC is the H-H elastic interaction term. T_c is the value of T for which there is a solution, at a specific C (the critical concentration), for the two constraints. $d\mu/dC=0$ and $d^2\mu/dC^2=0$. For $T_c=173$ °C, the corresponding value for u is 0.154 eV, while for $T_c=70$ °C it is 0.119 eV.

IV. CONCLUSIONS

Direct volumetric measurements conducted simultaneously with four-probe measurements serve as a simple, yet powerful, technique to study hydrogen absorption in thin metal films. Perhaps the most interesting result from the standpoint of hydrogen in metals is the enormous change in the phase diagram for hydrogen in thin films. There is evidence of the coexistence of a dilute phase (α) of hydrogen in the thin films, and a denser phase of hydrogen (α') which can exist up to [H]/[Nb]~0.7. In the thinnest films, the film expands normal to the film plane when loaded with hydrogen, with almost no lattice changes in the plane of the film. For films near 2000 Å an expansion is seen in the plane of the film with hydrogen loading.

The critical point in 200-Å layers is changed from 173 °C in the bulk to 70 °C. The modifications to the phase diagram are thought to be due to a clamping of the film to the substrate, and probably to a somewhat lesser extent the Pd overlayer. Clamping of the film is thought to weaken the elastic attractive interaction between hydrogen atoms, and this accounts for the drastic modification to the phase diagram. Of course, as the film becomes thicker complete clamping is not observed; some of these results have been discussed by others.[2–4]

The hydrogen chemical potential can be deduced for these Pd-covered films by studying the discharge of hydrogen for various oxygen pressures. For different oxygen pressures the interaction with atomic hydrogen, coming from the Nb to the Pd surface, can be measured with great precision, and even provides a way of studying the reaction kinetics. This work will be described elsewhere.[18] In general, hydrogen in these bilayers films provides a rich system for studying not only phase equilibria, but other related phenomena like the effect of large amounts of hydrogen on superconductivity.

ACKNOWLEDGMENTS

The preceding work was supported by the U.S. Department of Energy Division of Materials Sciences Contract No. DE-AC02-76CH0016 and BNL CRADA No. C-94-03. The authors are grateful for technical and scientific contributions from H. Wiesmann, F. Loeb, E. Gallego, Y. Gorelik, and T. Thurston. We thank V. Emery and P. Thomas for the useful discussions. The x-ray data were obtained at the BNL National Synchrotron Light Source (NSLS) which is also supported by the U.S. Department of Energy.

[1] H. Zabel and H. Peisl, Phys. Rev. Lett. **42**, 511 (1979).
[2] S. Blässer, J. Steiger, and A. Weidinger, Nucl. Instrum. Methods Phys. Res. Sect. B **85**, 24 (1994).
[3] J. Steiger, A. S. Blässer, O. Boebel, J. Erxmeyer, B. Mertesacker, and A. Weidinger, Z. Phys. Chem. **181**, 367 (1993).
[4] J. Steiger, A. S. Blässer, and A. Weidinger, Phys. Rev. B **49**, 5570 (1994).
[5] S. Moehlecke, C. F. Majkrzak, and Myron Strongin, Phys. Rev. B **31**, 6804 (1985).
[6] C. Moelle and H.-J. Fecht, Nanostruct. Mater. **3**, 93 (1993).
[7] P. F. Miceli, H. Zabel, and J. E. Cunningham, Phys. Rev. Lett. **54**, 917 (1985).
[8] P. M. Reimer, H. Zabel, C. P. Flynn, J. A. Matheny, K. Ritley, J. Steiger, S. Blässer, and A. Weidinger, Z. Phys. Chem. **181**, 367 (1993).
[9] M. A. Pick, J. W. Davenport, Myron Strongin, and G. J. Dienes, Phys. Rev. Lett. **43**, 286 (1979).
[10] Particle size was determined from broadening of the diffraction peaks. Details can be found in N. W. Jisrawi *et al.* (unpublished).
[11] J. D. Clewley, T. Curran, Ted B. Flanagan, and W. A. Oates, J. Chem. Soc. Faraday Trans. I **69**, 449 (1973).
[12] F. Seitz, *The Modern Theory of Solids*, 12th ed. (McGraw-Hill, New York, 1940), Chap. IV.
[13] G. Alefeld, Phys. Chem. **76**, 355 (1972).
[14] P. F. Miceli, H. Zabel, J. A. Dura, and C. P. Flynn, J. Mater. Res. **6**, 964 (1991).
[15] R. Feenstra, G. J. de Bruin-Hordijk, H. L. M. Bakker, R. Griessen, and D. G. de Groot, J. Phys. F **13**, L13 (1983).
[16] H. A. Goldberg. J. Phys. C **10**, 2059 (1977).
[17] G. Alefeld. Phys. Chem. **76**, 746 (1972).
[18] G. Reisfeld and M. Strongin, Chem. Phys. Lett. **246**, 85 (1995).